THE JOURNAL OF PHYSICAL CHEMISTRY A

Article

pubs.acs.org/JPCA

Molecular Docking toward Panchromatic Dye Sensitizers for Solar Cells Based upon Tetraazulenylporphyrin and Tetraanthracenylporphyrin

Cai-Rong Zhang,*[,†,‡] Xing-Yu Li,[†] Yu-Lin Shen,[§] You-Zhi Wu,[‡] Zi-Jiang Liu,[∥] and Hong-Shan Chen[⊥]

[†]School of Science and [‡]State Key Laboratory of Advanced Processing and Recycling of Non-ferrous Metals, Lanzhou University of Technology, Lanzhou, Gansu 730050, China

[§]Gansu Computing Center, Lanzhou 730000, China

[∥]Department of Physics, Lanzhou City University, Lanzhou 730070, China

[⊥]College of Physics and Electronic Engineering, Northwest Normal University, Lanzhou, Gansu 730070, China

Supporting Information

ABSTRACT: Novel dye sensitizers are highly expected in the development of dye-sensitized solar cells (DSSCs) because dye sensitizers can significantly affect the power conversion efficiency (PCE). Here, the molecular docking strategy is applied to design panchromatic dye sensitizers for DSSCs to improve light-harvesting efficiency covering the full solar spectrum. Considering the broad absorption bands of tetraanthracenylporphyrins (TAnPs) and tetraazuleneporphyrins (TAzPs), based upon porphyrin dye sensitizer YD2-o-C8, the panchromatic dye sensitizers coded as H_2(TAnP)-α, H_2(TAzP)-γ, H_2(TAzP)-ε, and H_2(TAzP)-δ are designed by the substitution of the porphyrin-ring in YD2-o-C8 with TAnPs and TAzPs moieties at different positions. The geometries, electronic structures, and excitation properties of the designed dye sensitizers are investigated using density functional theory (DFT) and time-dependent DFT methods. The analysis of geometries, conjugation lengths, electronic structures, absorption spectra, transition configurations, exciton binding energies, and free energy variations for electron injection and dye regeneration supports that the designed molecules are effective to be applied as potential candidates of dye sensitizers for DSSCs. Among the designed dye sensitizers, H_2(TAzP)-γ and H_2(TAnP)-α must have the better performance in DSSCs.

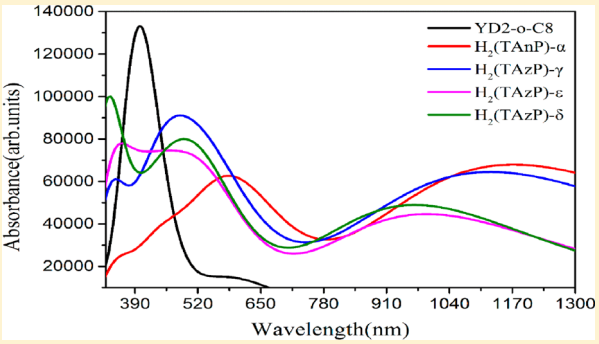

1. INTRODUCTION

Dye-sensitized solar cells (DSSCs) are developing as an alternative next-generation photovoltaic technologies for providing electricity at lower cost and relatively higher efficiency. In terms of electrons or holes as charge carriers, DSSCs are classified as n- and p-type. The incident photon to current conversion efficiency (IPCE) of n-type DSSCs is determined by the light-harvesting efficiency of dye sensitizers, the quantum yield of photoinduced electron injection (PIEI) and dye regeneration (DR), as well as the electron collection efficiency at the semiconductor electrode.[1] Apparently, dye sensitizers are very important in DSSCs due to its effects on light-harvesting, PIEI, and DR. Therefore, the design and development of novel dye sensitizers are an effective route to improve the power conversion efficiency (PCE) of DSSCs.[2]

Up to now, it has been recognized that the effective dye sensitizers usually have the following properties.[3] First, the wide absorption bands and large absorption coefficients are expected to harvest more photons from solar radiation. Also, the dye should have the suitable energy levels of the ground state (related to DR) and excited states with effective charge-transfer (CT) character which determines the PIEI mode in DSSCs.[4,5] In addition, the aggregation and recombination are expected to be suppressed in the molecular structure design for a dye sensitizer.[6,7] Consequently, all of the above-mentioned factors should be considered in the design and development of novel dye sensitizers for DSSCs.

Among the numerous reported dye sensitizers, porphyrin-based dye sensitizers are promising because their prominent performance in photosynthesis, optical absorbance, and other properties can be modified by their four *meso* and eight β reaction sites of the porphyrin ring.[8−10] For instance, the PCE about 12.3% was achieved from the DSSC sensitized by porphyrin dye sensitizer YD2-o-C8 with donor−π conjugate−acceptor (D−π−A) structure.[6] After that, the PCE up to 13% was reached by the DSSC based-upon a panchromatic porphyrin dye sensitizer SM315, containing a benzothiadiazole (BTD) moiety.[11]

Received: December 26, 2016
Revised: March 19, 2017
Published: March 20, 2017

DOI: 10.1021/acs.jpca.6b12979
J. Phys. Chem. A 2017, 121, 2655−2664

Porphyrin's absorption spectra possess intense Soret bands at about 400 nm and moderate Q bands at about 600 nm. The absorptions are limited to the UV−vis region without extending into the near-infrared (NIR) region. Because a large part of solar photon energy is in the NIR region,[12] the absorption ranges and intensities of porphyrin dye sensitizers are still insufficient,[13] and the panchromatic dye sensitizers are highly desired for more efficient DSSCs.[14,15] For instance, the carbazole fused thiophene-substituted zinc porphyrin dyes were developed to fill the absorption gap between the Soret and Q bands.[16] Thus, it is necessary to further improve light-harvesting abilities, shift absorption bands to the NIR region, broaden absorption bands, and increase extinction coefficients to develop panchromatic dye sensitizers for DSSCs.

The reported tetra(anthracenyl)porphyrins (TAnPs)[17] and tetra(azulene)porphyrins (TAzPs)[18] have intense absorptions covering the broad UV, visible, and NIR range revealed in the electronic absorption spectrum. On the basis of analysis of electronic structures and electronic absorption spectra, Jiang et al. found that the introduction of electron-withdrawing or electron-donating groups onto the periphery of the TAnP/TAzP skeleton can tune the gap between the highest occupied molecular orbital (HOMO) and the lowest unoccupied molecular orbital (LUMO), inducing an obvious shift of the absorption bands, and the introduction of electron-donating groups onto the periphery of anthracene at α positions and of azulene at ε positions (the positions are labeled in Figure 1) lead to novel panchromatic dyes.[19,20] This indicates that fusing anthracene/azulene to porphyrin core is effective to extend absorption into NIR region.

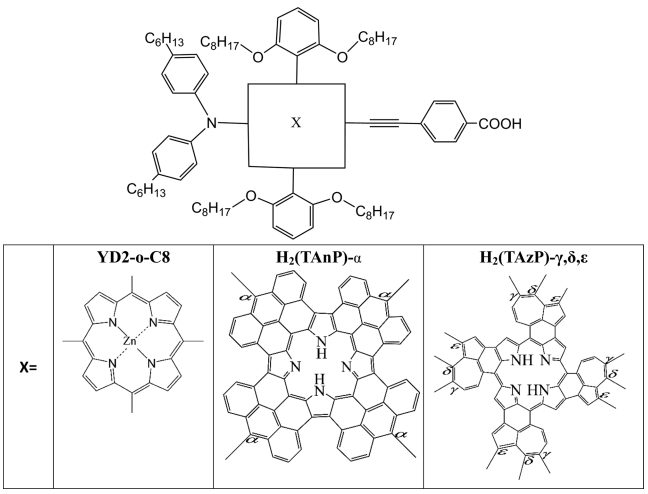

Figure 1. Molecular structures of YD2-o-C8 and the designed dye sensitizers H_2(TAnP)-α, H_2(TAzP)-γ, H_2(TAzP)-δ, and H_2(TAzP)-ε.

Usually, the porphyrin dye sensitizers applied in DSSCs have D−π−A structure. The absorption and electrochemical properties of porphyrin sensitizers can be tuned by modifying their donors,[21−24] conjugate bridges,[25−28] and acceptors.[29−31] For example, elongation of the π conjugation and loss of symmetry in porphyrins cause broadening and a red shift of the absorption bands together with an increasing intensity of the Q bands relative to that of the Soret bands.[32] Also, Lee et al. designed a series of porphyrin dye sensitizers with different electron donor and acceptor on the basis of quantum chemistry calculations and predicted some of designed dyes can be applied in DSSCs.[33]

The prominent performance of porphyrin dye sensitizers YD2-o-C8 (the molecular structure is shown in Figure 1) and SM315 in DSSCs underlines the possibility to learn the lessons from its molecular structure. The analysis of the molecular structure of YD2-o-C8 pointed out that the diarylamino (DAA) group with two hexyl chains and the phenylethynyl carboxylic acid (PECA) moiety act as electron donor and acceptor, respectively, whereas long alkoxyl chains in the ortho-positions of the meso-phenyls play the role of decreasing dye aggregation and blocking the approach of electrolyte molecules to electrode surface.[6] The electron donor and the role of porphyrin group in SM315 are same as that in YD2-o-C8, and the BTD moiety in SM315 plays the auxiliary electron acceptor.[34]

Because panchromatic and high performance dye sensitizers can be engineered by the combination of several chromophores into one dye molecule,[35] in this work, to design novel panchromatic dye sensitizers for DSSCs, we applied the molecular docking strategy in which we kept the prominent "gene" of YD2-o-C8, including D−π−A structure, donor, acceptor, and alkoxylphenyl moieties. Meanwhile, considering the effectiveness of panchromatic absorbance of TAnP and TAzP, the porphyrin ring in YD2-o-C8 is substituted with TAnP and TAzP. The designed dye sensitizers are labeled as H_2(TAnP)-α, H_2(TAzP)-γ, H_2(TAzP)-δ, and H_2(TAzP)-ε, respectively. The molecular structures of the designed dye sensitizers are presented in Figure 1, and the letters α, γ, δ, and ε represent the connecting position. The calculated geometries, electronic structures and excitation-related properties support that the designed dye sensitizers are potential candidates for DSSCs.

2. COMPUTATIONAL METHOD

The calculations for the ground state (geometry optimization and electronic structures) and excitation properties were conducted under the theoretical framework of density functional theory (DFT) and time-dependent DFT (TDDFT),[36−38] respectively. On the basis of the calculated results of excited states, the electronic absorption spectra were simulated using the Gaussian function. The Coulomb-attenuating long-range corrected hybrid functional CAM-B3LYP[39,40] was applied in DFT and TDDFT calculations because this functional is more suitable than other functionals to describe electronic structures and excitation properties of tetrahydroquinoline,[5] triphenylamine,[41] ethynyl-linked porphyrin−perylene arrays,[42] and porphyrin-based dye sensitizers.[7,43,44] The polarized split-valence basis sets 6-31G(d,p)[45] were selected because the basis sets are sufficient for calculating the excitation properties and electron density of organic dyes.[46,47] To compare the absorption spectra of the designed dye sensitizers with that of YD2-o-C8, the solvent effects were taken into account by using polarizable continuum model (PCM)[48] method with tetrahydrofuran (THF) solution in which the UV−vis absorption spectra of YD2-o-C8 dye sensitizer was measured. The DFT and TDDFT calculations were performed using Gaussian 09 package.[49]

In terms of the work principles of n-type DSSCs,[1] the important charge-transfer (CT) processes in DSSCs are PIEI from the excited dyes to semiconductor conduction band and the DR between the oxidized dye sensitizers and redox electrolyte. On the basis of the Marcus theory for electron transfer,[50] free energy variation is a significant factor to

DOI: 10.1021/acs.jpca.6b12979
J. Phys. Chem. A 2017, 121, 2655−2664

determine the rate constant of CT. According to Preat's method,[51] assuming PIEI occurs from the unrelaxed excited state of the dye, the free energy variation of the electron injection (ΔG^{inject}) can be calculated as the difference between the excited state oxidation potential (ESOP, E_{OX}^{dye*}) and the conduction band of semiconductor in electrode, whereas the free energy variation for DR (ΔG^{regen}) is the difference of the ground state redox potential (GSOP, E_{OX}^{dye}) between electrolyte and dye sensitizer. The E_{OX}^{dye} is obtained according to Koopman's theorem. The E_{OX}^{dye*} can be calculated as following[52]

$$E_{OX}^{dye*} = E_{OX}^{dye} - \lambda_{max} \quad (1)$$

in which the λ_{max} is the absorption maximum in electronvolts. The details of absorption spectra simulation and free energy variation were described in our previous work.[53] In this work, the conduction band of TiO_2 4.0 eV,[54] and the redox potential of iodide/triiodide redox couple 4.85 eV (0.35 V vs NHE)[55] are adopted for the calculation of free energy variation.

3. RESULTS AND DISCUSSION

3.1. Molecular Structures. The optimized geometrical structures of YD2-o-C8, H_2(TAnP), H_2(TAnP)-α, H_2(TAzP), H_2(TAzP)-γ, H_2(TAzP)-δ, and H_2(TAzP)-ε are presented in Figures S1−S7 in Supporting Information where the hydrogen atoms were omitted for clarity. The selected bond lengths, bond angles, and dihedral angles are listed in Tables S1 and S2 in the Supporting Information. For YD2-o-C8, the electron acceptor group PECA is coplanar with a porphyrin framework, and the dihedral angle between phenyl in the diarylamino and porphyrin framework (dihedral angle 19−21−26−28 is about 70°) indicates the remarkable torsion. The coplanar structure between electron acceptor and conjugate bridge is favorable for PIEI,[56] whereas the torsion between electron donor and conjugate bridge is propitious to form charge separated excited states.[57] H_2(TAnP) and H_2(TAzP) are butterfly-like structures. For H_2(TAnP), the four inner nitrogen atoms form a plane, while the torsion angle of 38−4−7−48 is about 16°, which can describe the angle between the adjacent anthracene units to some extent. However, the four inner nitrogen atoms in H_2(TAzP) are non-coplanar, the corresponding torsion angle is about 3°, and the torsion angles between azulene and pyrrole in porphyrin are larger than those between anthracene and pyrrole in the porphyrin of H_2(TAnP). For H_2(TAnP)-α, H_2(TAzP)-γ, H_2(TAzP)-δ, and H_2(TAzP)-ε, the corresponding geometric parameters, including bond lengths, bond angles, and dihedral angles, are quite similar due to the local character of formed chemical bonds. The remarkable difference in torsion angles between the phenyl in diarylamino and anthracene/azulene in π-conjugation results from the steric hindrance and substitution position effects. The quasi-planar structures between phenylethynyl carboxylic acid and the anthracene/azulene moiety in π-conjugation ensure effective electronic coupling and enhance electron delocalization. Also, it should be mentioned that, similarly to YD2-o-C8, the long alkoxyl chains in the ortho-positions of the meso-phenyls in designed dyes with large conjugation frameworks are very important for effective suppression of dye aggregation and blocking charge recombination. Furthermore, the nonplanar character of H_2(TAnP) and H_2(TAzP) groups in designed dyes is also favorable to hinder dye aggregation.

On the contrary, the conjugation length is closely related to the PCE of DSSCs.[5] It is reported that the electron-transfer rate for a series of rigid rodlike donor-bridge-acceptor compounds increases by a factor of 8 when the donor−acceptor distance is extended from 22.0 to 30.6 Å, and then it decreases by a factor of 188 when the distance is increased further to 39.2 Å.[58] This underlines the importance of donor−acceptor distance in the electron-transfer rate, and thus in the effects for the improvement of short-circuit current density (J_{SC}) in DSSCs. Here, we define the interatomic distance (IAD) between the N atom in diarylamino and the C atom in carboxylic acid for YD2-o-C8, H_2(TAnP)-α, H_2(TAzP)-γ, H_2(TAzP)-δ, and H_2(TAzP)-ε to describe conjugation length and donor−acceptor distance to some extent. The calculated IAD are about 16.6, 24.6, 23.3, 24.5, and 24.3 Å for YD2-o-C8, H_2(TAnP)-α, H_2(TAzP)-γ, H_2(TAzP)-δ, and H_2(TAzP)-ε, respectively. The IAD of H_2(TAnP)-α, H_2(TAzP)-γ, H_2(TAzP)-δ, and H_2(TAzP)-ε are similar to that of porphyrin dimmer sensitizer DTBC (about 25.0 Å).[43] In terms of the dependence of electron-transfer rate on donor−acceptor distance for a series of rigid rodlike donor−bridge−acceptor compounds,[58] analogously, the longer IAD of H_2(TAnP)-α, H_2(TAzP)-γ, H_2(TAzP)-δ, and H_2(TAzP)-ε may be favorable to improve the PIEI rate and J_{SC}. The longer IAD can also generate retardation in recombination dynamics between the injected electrons in electrode and the oxidized dye sensitizers.[2]

3.2. Electronic Structures. Analysis of electronic structures can help us to understand not only the energy level alignment relative to the conduction band of semiconductor in electrode and the redox potential of electrolyte but also the distribution of molecular orbital (MO) energies related to the density of states (DOS), as well as the oxidized and reduction potential of dye sensitizers. To compare conveniently, the frontier MO energies and HOMO−LUMO gaps (HLGs) of H_2(TAnP), H_2(TAnP)-α, H_2(TAzP), H_2(TAzP)-γ, H_2(TAzP)-δ, H_2(TAzP)-ε, and YD2-o-C8 dyes are presented Figure 2a−c. The energies of HOMO, LUMO, and HLG for H_2(TAnP) are −4.87, −2.48, and 2.39 eV, respectively. Introducing electron donor, acceptor, and terminal groups to H_2(TAnP), corresponding to H_2(TAnP)-α, results in an increase/decrease of the HOMO/LUMO to about 0.05/0.14 eV, giving a HLG about 2.20 eV. The slight change of HOMO indicates the weak electronic coupling between the introduced donor group and H_2(TAnP), and the remarkable change of LUMO and HLG result from the effective coupling between the introduced acceptor group and H_2(TAnP), enhancing electron delocalization. The HOMO/LUMO energies of H_2(TAzP) are lower/higher by about 0.22/0.11 eV than those of H_2(TAnP), respectively. This is attributed to the stabilization of electronic structures induced by more remarkable torsion between azulene units and lower symmetry of azulene. The HOMO/LUMO energies of H_2(TAzP)-γ (H_2(TAzP)-ε) are higher/lower by about 0.24/0.13 (0.01/0.07) eV than those of H_2(TAzP), respectively, whereas the HOMO/LUMO energy of H_2(TAzP)-δ is higher by about 0.05/0.02 eV than those of H_2(TAzP), respectively, suggesting the effective electronic coupling between the introduced groups and H_2(TAzP) at the γ position. Actually, the different torsion angle between the phenyl in diarylamino and azulene in π-conjugation (about 39°, 49°, and 53° for H_2(TAzP)-γ, H_2(TAzP)-δ, and H_2(TAzP)-ε, respectively) affects the extent of conjugation between electron donor DAA and H_2(TAzP), and thus the electronic coupling and HOMO energies. The comparison of electronic structures presented in Figure 2c gives the increase/decrease/reduction of the HOMO/LUMO/HLG of H_2(TAnP)-α, H_2(TAzP)-γ,

DOI: 10.1021/acs.jpca.6b12979
J. Phys. Chem. A 2017, 121, 2655−2664

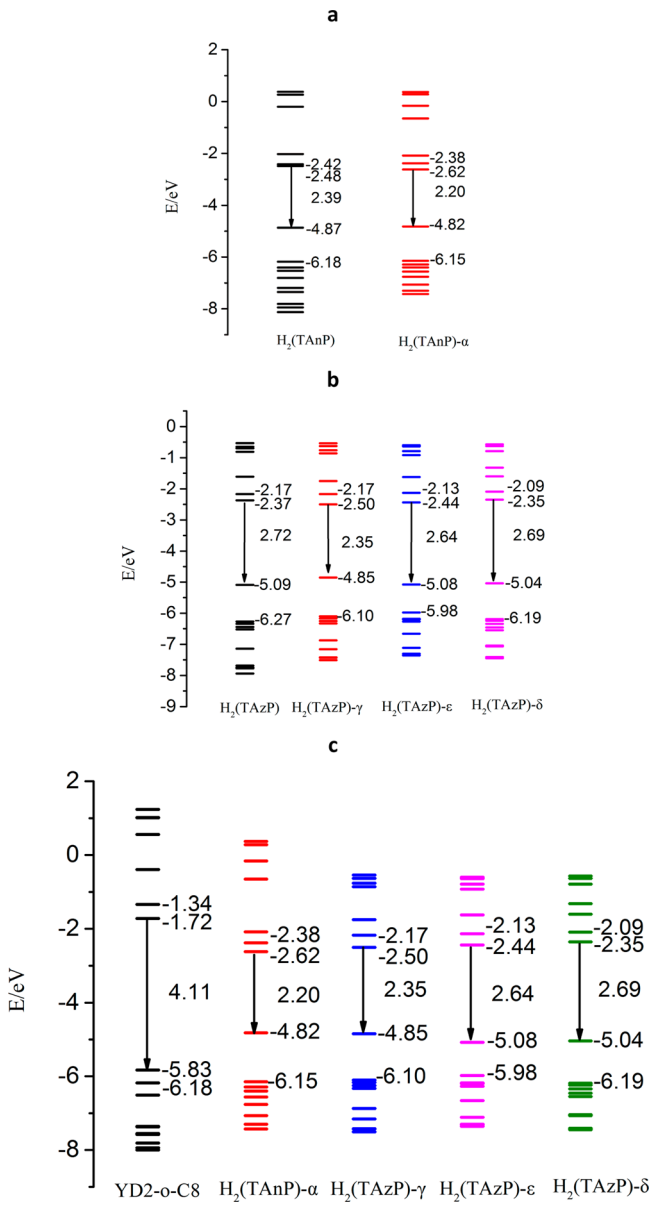

Figure 2. Calculated molecular orbital energies: (a) H_2(TAnP), H_2(TAnP)-α; (b) H_2(TAzP), H_2(TAzP)-γ, H_2(TAzP)-δ, and H_2(TAzP)-ε; (c) YD2-o-C8, H_2(TAnP)-α, H_2(TAzP)-γ, H_2(TAzP)-δ, and H_2(TAzP)-ε.

H_2(TAzP)-δ, and H_2(TAzP)-ε relative to those of YD2-o-C8, emphasizing the effectiveness of tuning electronic structures by substitution of porphyrin in YD2-o-C8 with H_2(TAnP)/H_2(TAzP), which extends the conjugation and enhances the electron delocalization though the coplanar structures of H_2(TAnP)/H_2(TAzP) in designed dyes are broken.

The analysis of electronic structures for organic and Ru complex dye sensitizers suggest that the dense distribution of MO eigenvalues near frontier MOs is favorable for J_{SC} improvement.[41,53,56,59,60] Figure 2c indicates that distribution of MO eigenvalues. In terms of the MOs from HOMO−1 to LUMO+1, the dense order of MO eigenvalues is H_2(TAnP)-α > H_2(TAzP)-ε > H_2(TAzP)-γ > H_2(TAzP)-δ > YD2-o-C8, meaning that the designed dye sensitizers may have larger J_{SC} values because the denser distribution of MO eigenvalues generates more absorption bands in NIR and UV−vis region.

The electronic structures of dye sensitizers also affect the open-circuit voltage (V_{OC}) of DSSCs. The V_{OC} can be calculated as[61]

$$V_{OC} = \frac{E_C + \Delta CB}{e} + \frac{kT}{e}\ln\left(\frac{n_C}{N_{CB}}\right) - \frac{E_{redox}}{e} \quad (2)$$

where e is the elementary charge, E_C is the conduction band edge of the semiconductor in the electrode of DSSCs, k is the Boltzmann constant, T is the absolute temperature, n_c is the number of electrons in the conduction band, N_{CB} is the density of accessible states in the conduction band, and E_{redox} is the reduction−oxidation potential of electrolyte in DSSCs. ΔCB is the shift of E_c induced by the dyes adsorption on semiconductor of electrode, and it can be estimated as[62]

$$\Delta CB = \frac{e\mu_{normal}\gamma}{\varepsilon\varepsilon_0} \quad (3)$$

In this formula, μ_{normal} denotes the dipole moment of individual dye molecules perpendicular to the surface of the semiconductor substrate, γ is the dye's surface concentration, and ε_0 and ε represent the vacuum permittivity and the relative dielectric permittivity, respectively. Considering the similarity of designed dye sensitizers, the γ values in eq 3 for the designed dyes should be similar, the main difference of ΔCB and the V_{OC} resulting from μ_{normal}. The calculated dipole moments of YD2-o-C8, H_2(TAnP)-α, H_2(TAzP)-γ, H_2(TAzP)-δ, and H_2(TAzP)-ε are about 3.86, 6.21, 13.41, 4.97, and 6.10 D, respectively. Therefore, the designed dye sensitizers H_2(TAnP)-α, H_2(TAzP)-γ, H_2(TAzP)-δ, and H_2(TAzP)-ε applied in DSSCs may induce larger ΔCB and thus the larger V_{OC} than that of YD2-o-C8.

3.3. Excitation Properties. The simulated absorption spectra are presented in Figure 3. It can be found from Figure 3a that, compared with the case for H_2(TAnP), the absorbance of H_2(TAnP)-α is significantly enhanced in the visible and NIR region, and the absorption bands in NIR region have a red shift. The absorbances of H_2(TAzP)-γ, H_2(TAzP)-δ, and H_2(TAzP)-ε relative to that of H_2(TAzP) exhibit similar tendencies, which are displayed in Figure 3b. Furthermore, the absorption spectra in Figure 3b show the substitution at the γ position is superior to those of δ and ε positions for enhancing absorption because of different extents of conjugation and electronic delocalization. The difference in absorption spectra of the designed dyes relative to H_2(TAnP)/H_2(TAzP) highlights the effects of molecular structure modification. Figure 3c indicates the absorbance of H_2(TAnP)-α, H_2(TAzP)-γ, H_2(TAzP)-δ, and H_2(TAzP)-ε are significantly enhanced relative to that of YD2-o-C8, and the absorption bands dramatically extend to the NIR region, indicating panchromatic absorption character. This supports the substitution of porphyrin in YD2-o-C8 with H_2(TAnP)/H_2(TAzP) as a successful strategy to expand absorption. In terms of the area under the absorption spectra profile, which can evaluate the light-harvesting efficiency to some extent, the absorbances of H_2(TAzP)-γ, H_2(TAzP)-δ, and H_2(TAzP)-ε are superior to that of H_2(TAnP)-α in the shorter wavelength region due to the difference of H_2(TAnP)/H_2(TAzP), whereas the absorbance of H_2(TAnP)-α is similar to that of H_2(TAzP)-γ in the longer wavelength region. Also, the different absorption properties in different wavelengths provides the possibility for cosensitization in DSSCs. Overall, the absorbance of H_2(TAzP)-γ is better than those of other designed dye sensitizers and YD2-o-C8.

DOI: 10.1021/acs.jpca.6b12979
J. Phys. Chem. A 2017, 121, 2655−2664

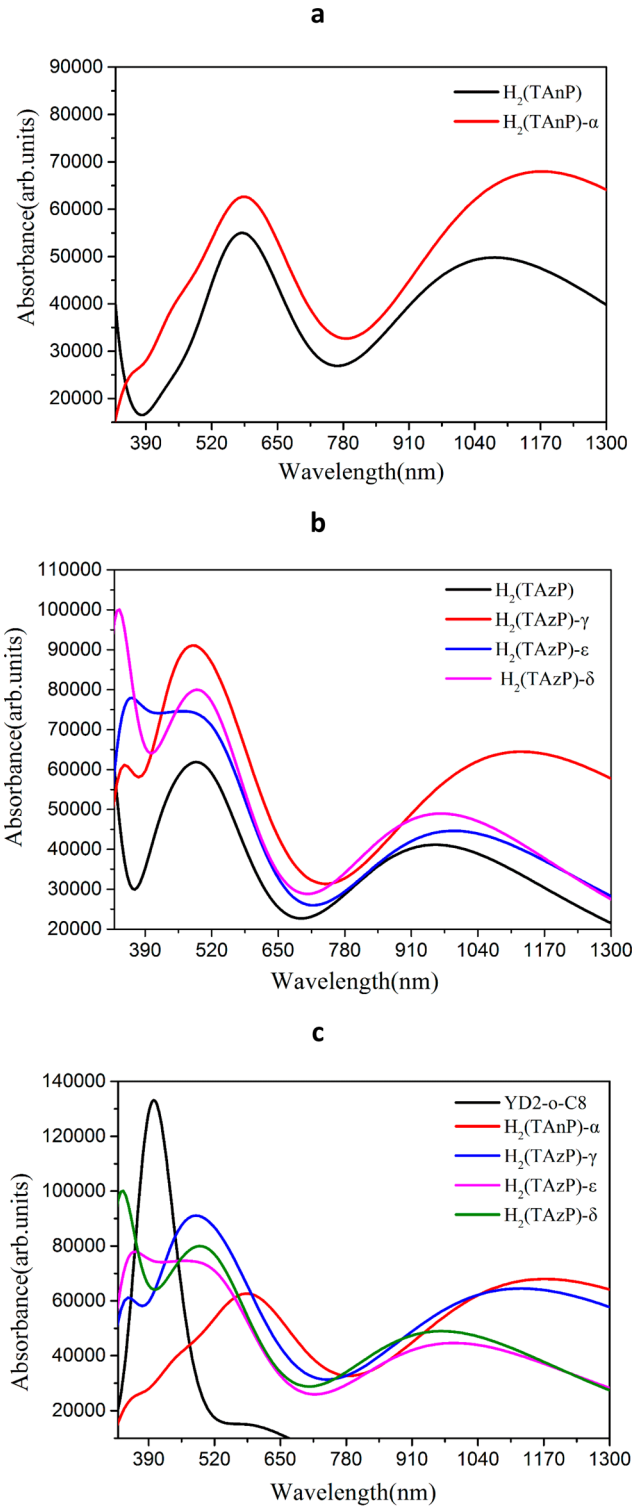

Figure 3. Simulated absorption spectra: (a) H_2(TAnP), H_2(TAnP)-α; (b) H_2(TAzP), H_2(TAzP)-γ, H_2(TAzP)-δ, and H_2(TAzP)-ε; (c) YD2-o-C8, H_2(TAnP)-α, H_2(TAzP)-γ, H_2(TAzP)-δ, and H_2(TAzP)-ε.

To understand the details of absorption spectra, we analyzed the excited states. Table 1 lists the singlet excited states of which the oscillator strengths are larger than 0.1 and the wavelengths are longer than 350 nm. The calculated excitation energies, corresponding wavelengths, oscillator strengths, and the major transition configurations (coefficients >10%) are given in the table. The data in Table 1 indicate that the oscillator strength of S_1 states for H_2(TAnP)-α, H_2(TAzP)-γ, H_2(TAzP)-δ, and H_2(TAzP)-ε are remarkably larger than those of YD2-o-C8, H_2(TAnP), and H_2(TAzP), suggesting the effectiveness of absorption enhancement using D−π−A structure and fusing anthracene/azulene to the porphyrin core. Furthermore, the numbers of excited states with an excitation wavelength in the visible and NIR region for H_2(TAnP)-α, H_2(TAzP)-γ, H_2(TAzP)-δ, and H_2(TAzP)-ε are quite larger than that of YD2-o-C8, meaning more excited states for PIEI. To further understand the transition character (local or CT excitations) of the designed dyes, we analyzed the related MOs that are given in Tables S3−S5 in the Supporting Information. The HOMO−2 and HOMO−1 of H_2(TAnP) and H_2(TAzP) show localized character, whereas the other MOs for H_2(TAnP) and H_2(TAzP) are delocalized. For YD2-o-C8, the HOMO−2 and HOMO are contributed by DAA, porphyrin, and the phenylethynyl moiety, whereas the HOMO−1 and LUMO+1 are localized in porphyrin and LUMO, LUMO+2, and LUMO+3 involve the porphyrin and PECA. For H_2(TAnP)-α, LUMO and LUMO+2 extend from H_2TAnP to the ethynyl moiety, whereas LUMO+1 is localized in H_2TAnP and LUMO+3 and LUMO+4 are mainly contributed by the composition of H_2TAnP and PECA. Meanwhile, the LUMO+2 of H_2(TAzP)-δ, the LUMO+3 of H_2(TAzP)-ε and H_2(TAzP)-δ, the LUMO+4 of H_2(TAzP)-γ, the LUMO+5 of H_2(TAzP)-ε, and the LUMO+7 of H_2(TAzP)-γ, H_2(TAzP)-δ, and H_2(TAzP)-ε contain the remarkable contribution from PECA and part of H_2(TAzP). However, the other unoccupied MOs related to the transitions for H_2(TAzP)-γ, H_2(TAzP)-δ, and H_2(TAzP)-ε are localized in different parts of H_2(TAzP). Apparently, the MO relocations between the initial and final states for a transition indicate CT character. It is reported that there are three kinds of PIEI modes at different time scales in DSSCs with YDoc.[4] Similarly, for the designed dye sensitizers H_2(TAnP)-α, H_2(TAzP)-γ, H_2(TAzP)-δ, and H_2(TAzP)-ε, if the MOs involved in the final state of transition extend to the acceptor/anchor group (PECA moiety for these dyes), PIEI is the fast mode; otherwise, PIEI is the slow mode. For instance, PIEI of S1 state for H_2(TAzP)-δ is the slow mode because the LUMO involved in the S1 transition is localized in H_2(TAzP). Therefore, according to the MOs involved in the final state, the transitions in NIR for the designed dye sensitizers are slow modes for PIEI, whereas the fast modes for PIEI are related to the excited transitions in the visible region.

The exciton binding energy (EBE) can determine the efficiency of charge separation in solar cells.[63] The EBE can be calculated as the energy difference between the electronic and optical band gap.[64] The electronic band gap is approximated as the HLG for dye sensitizers, whereas the first excitation energy is adopted as the optical gap.[63,65] The calculated EBE (in eV) for YD2-o-C8, H_2(TAnP)-α, H_2(TAzP)-γ, H_2(TAzP)-δ, and H_2(TAzP)-ε are 2.01, 1.21, 1.33, 1.49, and 1.48 eV, respectively. The smaller EBE is favorable for exciton dissociation and generating free charge carriers in DSSCs, resulting in smaller energy barriers for electron injection. Therefore, compared with YD2-o-C8, the smaller EBEs for the designed dye sensitizers are a positive factor to improve PIEI efficiency. The inverse correlation between EBE and the light-harvesting efficiency (LHE) implies that the dyes with lower EBE produce more efficient light harvesting.[5] This means the designed dye sensitizers are more efficient for light harvesting than YD2-o-C8. The tendency agrees with that of the simulated absorption spectra.

DOI: 10.1021/acs.jpca.6b12979
J. Phys. Chem. A 2017, 121, 2655−2664

Table 1. Calculated Excitation Energies and Corresponding Wavelengths (λ), Oscillator Strengths ($f > 0.1$), and Major Transition Configurations with Coefficients Larger Than 10%

dyes	states	majortransition configurations	λ (eV/nm)	f
H_2(TAnP)	S_1	(94%)H→L	1.13/1095	0.6600
	S_2	(93%)H→L+1	1.14/1086	0.5395
	S_4	(87%)H−1→L	2.05/606	0.6461
	S_5	(85%)H−1→L+1	2.11/587	0.4331
	S_8	(61%)H−4→L+1; (30%)H−2→L+2	2.34/531	0.2977
	S_{11}	(40%)H−3→L+2; (31%)H−6→L; (14%)H−4→L	2.75/451	0.3082
	S_{14}	(54%)H−5→L; (21%)H−2→L+2; (13%)H−4→L+1	3.00/414	0.1174
H_2(TAnP)-α	S_1	(95%)H→L	0.99/1257	1.0576
	S_2	(91%)H→L+1	1.14/1083	0.6407
	S_3	(96%)H→L+2	1.46/850	0.1010
	S_4	(85%)H−1→L	1.93/641	0.5894
	S_6	(78%)H−1→L+1	2.10/590	0.5184
	S_8	(23%)H−5→L; (18%)H−5→L+1; (16%)H−2→L+2; (10%)H−1→L+2	2.25/552	0.2052
	S_9	(30%)H−2→L+1; (23%)H−1→L+2; (10%)H−2→L	2.28/544	0.1287
	S_{12}	(21%)H−4→L; (17%)H−4→L+2; (17%)H−3→L+2	2.67/465	0.4137
	S_{15}	(59%)H−6→L; (11%)H−5→L+1	2.85/435	0.1348
	S_{16}	(76%)H→L+3; (14%)H→L+4	2.93/423	0.1580
	S_{22}	(65%)H→L+4	3.32/374	0.1232
	S_{30}	(14%)H−15→L+1; (10%)H−16→L+2; (10%)H→L+6	3.50/355	0.1132
H_2(TAzP)	S_1	(84%) H→L	1.22/1015	0.5274
	S_2	(78%)H→L+1	1.33/930	0.4680
	S_6	(34%)H−3→L; (18%)H−1→L	2.06/603	0.1330
	S_8	(60%)H−1→L; (11%)H→L+1	2.30/539	0.5557
	S_{10}	(28%)H−1→L+1; (24%)H−3→L+1; (11%)H→L+5	2.44/508	0.4116
	S_{12}	(25%)H−3→L; (23%)H→L+4; (14%)H→L+5	2.53/490	0.1038
	S_{13}	(31%)H−3→L+1; (19%)H→L+4; (15%)H→L+5	2.70/460	0.3215
	S_{15}	(52%)H−4→L+1; (12%)H→L+6; (11%)H−4→L	2.81/440	0.1086
	S_{16}	(46%)H−5→L; (13%)H→L+5; (11%)H−3→L	2.94/422	0.4623
	S_{18}	(37%)H−5→L+1; (15%)H−2→L+2; (10%)H−3→L+1	3.21/386	0.1757
H_2(TAzP)-γ	S_1	(91%)H→L	1.02/1220	1.0426
	S_2	(82%)H→L+1	1.19/1039	0.5354
	S_3	(60%)H→L+2; (11%)H−2→L+1	1.53/811	0.2582
	S_7	(30%)H−1→L; (28%)H→L+2	2.04/609	0.2033
	S_8	(25%)H−1→L; (21%)H−4→L; (14%)H−2→L	2.15/576	0.5010
	S_{10}	(25%)H→L+5; (19%)H−2→L; (17%)H→L+4	2.35/527	0.2634
	S_{11}	(54%)H→L+3	2.35/527	0.1620
	S_{12}	(34%)H−4→L+1; (12%)H−3→L+1; (10%)H→L+6	2.39/519	0.4411
	S_{14}	(31%)H→L+6; (14%)H−5→L; (11%)H−4→L	2.60/476	0.2056
	S_{15}	(20%)H−3→L+1; (14%)H−4→L+1; (13%)H→L+5	2.65/467	0.3270
	S_{16}	(19%)H−5→L; (16%)H−4→L+1; (15%)H−1→L+2; (11%)H−1→L+1	2.76/450	0.2876
	S_{17}	(25%)H−8→L; (12%)H−5→L; (10%)H−3→L+1	2.80/443	0.4968
	S_{18}	(11%)H−2→L+3; (10%)H−8→L; (10%)H−6→L+2	2.97/417	0.2688
	S_{19}	(23%)H→L+7; (16%)H→L+4	3.02/411	0.1295
	S_{26}	(16%)H→L+7	3.34/372	0.1928
H_2(TAzP)-ε	S_1	(86%)H→L	1.16/1072	0.6398
	S_2	(77%)H→L+1	1.32/940	0.4486
	S_3	(38%)H→L+2; (22%)H−1→L; (11%)H−2→L+1	1.60/775	0.1032
	S_7	(29%)H→L+2; (19%)H−3→L; (13%)H−4→L; (11%)H−1→L	2.19/565	0.3415
	S_8	(50%)H−3→L; (16%)H→L+2	2.21/560	0.4514
	S_{10}	(15%)H−4→L+1; (11%)H→L+5	2.40/517	0.1565
	S_{11}	(14%)H−3→L+1; (13%)H→L+6; (12%)H−5→L	2.42/512	0.4146
	S_{15}	(24%)H−5→L; (23%)H−1→L+1; (13%)H→L+3; (11%)H−4→L+1	2.72/457	0.1881
	S_{16}	(18%)H−5→L; (26%)H−4→L+1; (19%)H→L+6	2.76/449	0.4633
	S_{17}	(26%)H−4→L+2; (19%)H−3→L+2; (18%)H−6→L	2.94/422	0.2716
	S_{18}	(31%)H−3→L+2	2.95/420	0.1864
	S_{19}	(37%)H−5→L+1	3.09/401	0.1276
	S_{21}	(26%)H→L+5	3.19/389	0.3847
	S_{24}	(15%)H→L+6	3.31/374	0.1008

DOI: 10.1021/acs.jpca.6b12979
J. Phys. Chem. A 2017, 121, 2655−2664

Table 1. continued

dyes	states	majortransition configurations	λ (eV/nm)	f
	S_{25}	(27%)H−2→L+2	3.36/369	0.1055
	S_{28}	(32%)H−11→L; (11%)H−4→L+3	3.51/354	0.1297
H_2(TAzP)-δ	S_1	(87%)H→L	1.20/1033	0.6965
	S_2	(79%)H→L+1	1.34/926	0.4955
	S_3	(53%)H→L+2 ; (15%)H−2→L+1; (11%)H−4→L	1.68/739	0.1140
	S_7	(35%)H−1→L; (18%)H→L+3; (10%)H−4→L	2.22/559	0.4272
	S_8	(26%)H−4→L; (29%)H→L+2	2.29/542	0.1300
	S_9	(22%)H−2→L; (18%)H−1→L; (15%)H→L+3; (14%)H−2→L+1; (10%)H−3→L	2.31/536	0.1619
	S_{10}	(51%)H−2→L; (17%)H−3→L; (15%)H→L+3	2.36/524	0.1367
	S_{11}	(28%)H−1→L+1; (18%)H→L+5; (13%)H−3→L+1	2.43/511	0.5471
	S_{14}	(28%)H−3→L+1; (18%)H→L+5; (13%)H−6→L	2.69/462	0.3028
	S_{15}	(45%)H−5→L	2.74/452	0.1677
	S_{16}	(34%)H−4→L+1; (10%)H→L+6	2.83/438	0.2777
	S_{17}	(19%)H−6→L; (12%)H−6→L+1; (11%)H→L+2	2.86/434	0.3301
	S_{18}	(43%)H−1→L+2; (20%)H−4→L+1	3.02/411	0.1004
	S_{19}	(21%)H−4→L+3; (15%)H−6→L	3.12/398	0.1469
	S_{20}	(27%)H−6→L+1; (14%)H→L+5; (19%)H−2→L+2; (12%)H−3→L+1	3.25/382	0.1899
	S_{22}	(20%)H−5→L+4; (10%)H−3→L+4	3.33/372	0.2425
	S_{23}	(14%)H−1→L+3; (12%)H→L+5	3.37/368	0.1124
YD2-o-C8	S_1	(73%)H→L; (23%)H−1→L+1	2.10/592	0.3470
	S_3	(53%)H−2→L; (25%)H−1→L+1; (12%)H→L	2.82/439	0.3594
	S_4	(43%)H−1→L; (54%)H→L+1	3.07/404	1.1081
	S_5	(28%)H−2→L; (52%)H−1→L+1; (11%)H→L	3.12/397	1.8676
	S_6	(90%)H−2→L+1	3.50/354	0.2715

The excitation properties of dye sensitizers can affect the J_{SC}, which is an important parameter to evaluate the performance of DSSCs. The formula to calculate J_{SC} is the following,[1]

$$J_{SC} = \int e\mathrm{LHE}(\lambda)\, \varphi_{inj}(\lambda)\, \varphi_{reg}\eta_{CC}(\lambda)\, \phi_{ph,AM1.5G}(\lambda)\, d\lambda \quad (4)$$

where e is the elementary charge and $\phi_{ph,AM1.5G}(\lambda)$ is the photon flux in AM1.5G, LHE is the light-harvesting efficiency (LHE = $1-10^{-A}$, with A being the absorbance coefficient), φ_{inj} and φ_{reg} are the quantum yields for electron injection and dye regeneration, respectively, and η_{CC} is the charge collection efficiency. In eq 4, $\phi_{ph,AM1.5G}(\lambda)$ and η_{CC} are determined by the light source and electrode in DSSC, respectively, LHE and φ_{inj} are decided by the electronic structures of the dyes' excited states, and φ_{reg} is influenced by the ground state electronic structures of dye sensitizers. In terms of simulated absorption spectra, the LHE of the designed dyes are superior to that of YD2-o-C8 for harvesting photon energies. More precisely, φ_{inj} depend on the dyes' excited state characters, excited states lifetimes, and the number of excited states in the investigated wavelength region. The more excited states for the designed dyes in the visible and NIR regions are favorable to increase φ_{inj}. Therefore, LHE and φ_{inj} of the designed dyes are the advantages to improve J_{SC}'s of DSSCs.

3.4. Free Energy Variations. The ESOP (E^*_{OX}, in eV), ΔG^{inject} (in eV) and ΔG^{regen} (in eV) for YD2-o-C8, H_2(TAnP)-α, H_2(TAzP)-γ, H_2(TAzP)-δ, and H_2(TAzP)-ε are listed Table 2. The similar E^*_{OX} values of H_2(TAnP)-α, H_2(TAzP)-γ, and H_2(TAzP)-δ are larger by about 0.10 eV than that of YD2-o-C8, and smaller by about 0.09 eV than that of H_2(TAzP)-ε. In terms of the calculation method for E^*_{OX}, the largest $E^*_{OX}$of H_2(TAzP)-ε results from its GSOP and the excitation energy of the S1 state. All of the ΔG^{inject} for these dyes are negative. This means that the energies of dyes' excited states in NIR excitations lie above the TiO_2 conduction band edge, inducing energetically permitted PIEI in DSSCs. Also, compared with the case for YD2-o-C8, the absolute values of ΔG^{inject} for the designed dyes are smaller, generating a negative impact on PIEI. However, considering the ΔG^{inject} in Table 2 calculated for the S1 state, the other excited states must have larger absolute values of ΔG^{inject}, which is favorable for fast PIEI. Furthermore, all of the ΔG^{regen} for these dyes are positive, indicating energetically permitted dye regeneration. Compared with the case for YD2-o-C8, the smaller ΔG^{regen} for H_2(TAnP)-α, H_2(TAzP)-γ, H_2(TAzP)-δ, and H_2(TAzP)-ε reduce the driving force for dye regeneration.

Table 2. Calculated Excited States Oxidized Potential (E^*_{OX}, eV), Free-Energy Variation for Electron Injection ΔG^{inject} (eV), and Free-Energy Variation for Dye Regeneration ΔG^{regen} (eV) for YD2-o-C8, H_2(TAnP)-α, H_2(TAzP)-γ, H_2(TAzP)-δ, and H_2(TAzP)-ε

dyes	E^*_{OX}	ΔG^{inject}	ΔG^{regen}
YD2-o-C8	3.73	−0.27	1.03
H_2(TAnP)-α	3.83	−0.17	0.02
H_2(TAnP)-γ	3.83	−0.17	0.05
H_2(TAzP)-ε	3.92	−0.08	0.28
H_2(TAzP)-δ	3.84	−0.16	0.24

4. CONCLUSIONS

In this work, we designed four kinds of panchromatic dye sensitizers for DSSCs, coded as H_2(TAnP)-α, H_2(TAzP)-γ, H_2(TAzP)-δ, and H_2(TAzP)-ε, using the molecular docking strategy. Concretely, on the basis of the prominent porphyrin dye sensitizer YD2-o-C8, we substitute the porphyrin ring in YD2-o-C8 at different positions with TAnPs and TAzPs moieties. The geometries, electronic structures, and excitation properties of the designed dye sensitizers are investigated using DFT and TDFT methods. From the geometric parameters, the

DOI: 10.1021/acs.jpca.6b12979
J. Phys. Chem. A 2017, 121, 2655−2664

longer IAD of the designed dyes is a positive factor to improve the PIEI rate and J_{SC}. The results of electronic structures suggest that, compared with the case for YD2-o-C8, the reduced HLGs, the denser distributions of MO eigenvalues, the smaller EBEs, and the larger dipole moments for the designed dyes are favorable to improve J_{SC} and V_{OC}. The absorption spectra of the designed dyes exhibit panchromatic character and show significant enhancement compared with that of YD2-o-C8. The analysis of transition configurations indicates that the transitions in NIR for the designed dye sensitizers are slow modes for PIEI, whereas the fast modes for PIEI are related to the excited transitions in visible region, and the LHE and φ_{inj} of the designed dyes are the advantages to improve J_{SC}. The results of the ΔG^{inject} and ΔG^{regen} for these dyes mean that PIEI and DR in DSSCs are energetically permitted. Therefore, the results of this work support that the designed molecules are effective to be applied as potential candidates of dye sensitizers for DSSCs, and the performance of H_2(TAzP)-γ and H_2(TAnP)-α must be better than those of other designed dye sensitizers. We expect that the experimental study can test the effectiveness of the designed dye sensitizers in DSSCs. If necessary, the electronic structures and properties of the designed dye sensitizers can be tuned further by introducing metal center (similar to Zn in prophyrin dyes) and auxiliary electron acceptor (such as the BTD moiety in porphyrin dye sensitizer SM315).

■ ASSOCIATED CONTENT

Supporting Information

The Supporting Information is available free of charge on the ACS Publications website at DOI: 10.1021/acs.jpca.6b12979.

Optimized molecular structures, the selected geometrical parameters, and the molecular orbitals of YD2-o-C8, H_2(TAnP), H_2(TAzP), H_2(TAnP)-α, H_2(TAzP)-γ, H_2(TAzP)-ε, and H_2(TAzP)-δ (PDF)

■ AUTHOR INFORMATION

Corresponding Author

*Tel: +86 0931 2973780. Fax: +86 0931 2976040. E-mail address: zhcrxy@lut.cn (C. R. Zhang).

ORCID

Cai-Rong Zhang: 0000-0002-4067-2798

Notes

The authors declare no competing financial interest.

■ ACKNOWLEDGMENTS

This work was supported by the National Natural Science Foundation of China (Grant No. 11164016). The authors were grateful to the high performance computing platform of Lanzhou University of Technology and the National Supercomputing Center in Shenzhen.

■ REFERENCES

(1) Hagfeldt, A.; Boschloo, G.; Sun, L.; Kloo, L.; Pettersson, H. Dye-Sensitized Solar Cells. *Chem. Rev.* **2010**, *110* (11), 6595−6663.

(2) Clifford, J. N.; Martinez-Ferrero, E.; Viterisi, A.; Palomares, E. Sensitizer molecular structure-device efficiency relationship in dye sensitized solar cells. *Chem. Soc. Rev.* **2011**, *40* (3), 1635−1646.

(3) Gratzel, M. Recent advances in sensitized mesoscopic solar cells. *Acc. Chem. Res.* **2009**, *42* (11), 1788−1798.

(4) Ju, M.-G.; Liang, W. Computational Insight on the Working Principles of Zinc Porphyrin Dye-Sensitized Solar Cells. *J. Phys. Chem. C* **2013**, *117* (29), 14899−14911.

(5) Zhang, C.-R.; Liu, L.; Zhe, J.-W.; Jin, N.-Z.; Ma, Y.; Yuan, L.-H.; Zhang, M.-L.; Wu, Y.-Z.; Liu, Z.-J.; Chen, H.-S. The Role of the Conjugate Bridge in Electronic Structures and Related Properties of Tetrahydroquinoline for Dye Sensitized Solar Cells. *Int. J. Mol. Sci.* **2013**, *14* (3), 5461−5481.

(6) Yella, A.; Lee, H. W.; Tsao, H. N.; Yi, C. Y.; Chandiran, A. K.; Nazeeruddin, M. K.; Diau, E. W. G.; Yeh, C. Y.; Zakeeruddin, S. M.; Gratzel, M. Porphyrin-Sensitized Solar Cells with Cobalt (II/III)-Based Redox Electrolyte Exceed 12% Efficiency. *Science* **2011**, *334* (6056), 629−634.

(7) Han, L.-H.; Zhang, C.-R.; Zhe, J.-W.; Jin, N.-Z.; Shen, Y.-L.; Wang, W.; Gong, J.-J.; Chen, Y.-H.; Liu, Z.-J. Understanding the Electronic Structures and Absorption Properties of Porphyrin Sensitizers YD2 and YD2-o-C8 for Dye-Sensitized Solar Cells. *Int. J. Mol. Sci.* **2013**, *14* (10), 20171−20188.

(8) Li, L.-L.; Diau, E. W.-G. Porphyrin-sensitized solar cells. *Chem. Soc. Rev.* **2013**, *42* (1), 291−304.

(9) Ishida, M.; Park, S. W.; Hwang, D.; Koo, Y. B.; Sessler, J. L.; Kim, D. Y.; Kim, D. Donor-Substituted β-Functionalized Porphyrin Dyes on Hierarchically Structured Mesoporous TiO_2 Spheres. Highly Efficient Dye-Sensitized Solar Cells. *J. Phys. Chem. C* **2011**, *115* (39), 19343−19354.

(10) Higashino, T.; Imahori, H. Porphyrins as Excellent Dyes for Dye-sensitized Solar Cells: Recent Developments and Insights. *Dalton Trans.* **2015**, *44* (2), 448−463.

(11) Mathew, S.; Yella, A.; Gao, P.; Humphry-Baker, R.; Curchod, B. F.; Ashari-Astani, N.; Tavernelli, I.; Rothlisberger, U.; Nazeeruddin, M. K.; Gratzel, M. Dye-sensitized Solar Cells with 13% Efficiency Achieved through the Molecular Engineering of Porphyrin Sensitizers. *Nat. Chem.* **2014**, *6* (3), 242−247.

(12) Qi, D.; Zhang, L.; Zhang, Y.; Bian, Y.; Jiang, J. Nature of the Intense Near-IR Absorption and Unusual Broad UV-Visible-NIR Spectra of Azulenocyanines: Density Functional Theory Studies. *J. Phys. Chem. A* **2010**, *114* (51), 13411−13417.

(13) Liu, J.; Liu, B.; Tang, Y.; Zhang, W.; Wu, W.; Xie, Y.; Zhu, W.-H. Highly Efficient Cosensitization of D−A−π−A Benzotriazole Organic Dyes with Porphyrin for Panchromatic Dye-sensitized Solar Cells. *J. Mater. Chem. C* **2015**, *3* (42), 11144−11150.

(14) Imahori, H.; Umeyama, T.; Ito, S. Large pi-Aromatic Molecules as Potential Sensitizers for Highly Efficient Dye-Sensitized Solar Cells. *Acc. Chem. Res.* **2009**, *42* (11), 1809−1818.

(15) Shi, Y.; Hill, R. B.; Yum, J. H.; Dualeh, A.; Barlow, S.; Gratzel, M.; Marder, S. R.; Nazeeruddin, M. K. A High-efficiency Panchromatic Squaraine Sensitizer for Dye-sensitized Solar Cells. *Angew. Chem., Int. Ed.* **2011**, *50* (29), 6619−6621.

(16) Zhao, L.; Wagner, P.; van der Salm, H.; Clarke, T. M.; Gordon, K. C.; Mori, S.; Mozer, A. J. Dichromophoric Zinc Porphyrins: Filling the Absorption Gap between the Soret and Q Bands. *J. Phys. Chem. C* **2015**, *119* (10), 5350−5363.

(17) Davis, N. K. S.; Thompson, A. L.; Anderson, H. L. A Porphyrin Fused to Four Anthracenes. *J. Am. Chem. Soc.* **2011**, *133* (1), 30−31.

(18) Kurotobi, K.; Kim, K. S.; Noh, S. B.; Kim, D.; Osuka, A. A Quadruply Azulene-fused Porphyrin with Intense Near-IR Absorption and a Large Two-photon Absorption Cross Section. *Angew. Chem., Int. Ed.* **2006**, *45* (24), 3944−3947.

(19) Qi, D.; Jiang, J. Toward Panchromatic Organic Functional Molecules: Density Functional Theory Study on the Electronic Absorption Spectra of Substituted Tetraanthracenylporphyrins. *J. Phys. Chem. A* **2011**, *115* (47), 13811−13820.

(20) Qi, D.; Zhang, L.; Jiang, J. Toward Panchromatic Organic Functional Molecules: Density Functional Theory Study on the Nature of the Broad UV-Vis-NIR Spectra of Substituted Tetra-(azulene)porphyrins. *J. Mol. Graphics Modell.* **2012**, *38*, 304−313.

(21) Wu, C.-H.; Pan, T.-Y.; Hong, S.-H.; Wang, C.-L.; Kuo, H.-H.; Chu, Y.-Y.; Diau, E. W.-G.; Lin, C.-Y. A Fluorene-modified Porphyrin

DOI: 10.1021/acs.jpca.6b12979
J. Phys. Chem. A 2017, 121, 2655−2664

for Efficient Dye-sensitized Solar Cells. *Chem. Commun.* **2012**, *48* (36), 4329−4331.
(22) Liu, B.; Zhu, W.; Wang, Y.; Wu, W.; Li, X.; Chen, B.; Long, Y.-T.; Xie, Y. Modulation of Energy Levels by Donor Groups: an Effective Approach for Optimizing the Efficiency of Zinc-porphyrin Based Solar Cells. *J. Mater. Chem.* **2012**, *22* (15), 7434−7444.
(23) Ambre, R. B.; Chang, G. F.; Zanwar, M. R.; Yao, C. F.; Diau, E. W. G.; Hung, C. H. New Dual Donor-Acceptor (2D-2A) Porphyrin Sensitizers for Stable and Cost-Effective Dye-Sensitized Solar Cells. *Chem. - Asian J.* **2013**, *8* (9), 2144−2153.
(24) Kang, M. S.; Choi, I. T.; Kim, Y. W.; You, B. S.; Kang, S. H.; Hong, J. Y.; Ju, M. J.; Kim, H. K. Novel D-pi-A structured Zn(II)-porphyrin Dyes with Bulky Fluorenyl Substituted Electron Donor Moieties for Dye-sensitized Solar Cells. *J. Mater. Chem. A* **2013**, *1* (34), 9848−9852.
(25) Liu, Y. Z.; Lin, H.; Dy, J. T.; Tamaki, K.; Nakazaki, J.; Nakayama, D.; Uchida, S.; Kubo, T.; Segawa, H. N-fused Carbazole-zinc Porphyrin-free-base Porphyrin Triad for Efficient Near-IR Dye-sensitized Solar Cells. *Chem. Commun.* **2011**, *47* (13), 4010−4012.
(26) Barea, E. M.; Caballero, R.; López-Arroyo, L.; Guerrero, A.; de la Cruz, P.; Langa, F.; Bisquert, J. Triplication of the Photocurrent in Dye Solar Cells by Increasing the Elongation of the π-conjugation in Zn-Porphyrin Sensitizers. *ChemPhysChem* **2011**, *12* (5), 961−965.
(27) Chang, Y.-C.; Wang, C.-L.; Pan, T.-Y.; Hong, S.-H.; Lan, C.-M.; Kuo, H.-H.; Lo, C.-F.; Hsu, H.-Y.; Lin, C.-Y.; Diau, E. W.-G. A Strategy to Design Highly Efficient Porphyrin Sensitizers for Dye-sensitized Solar Cells. *Chem. Commun.* **2011**, *47* (31), 8910−8912.
(28) Xiang, N.; Huang, X. W.; Feng, X. M.; Liu, Y. J.; Zhao, B.; Deng, L. J.; Shen, P.; Fei, J. J.; Tan, S. T. The Structural Modification of Thiophene-linked Porphyrin Sensitizers for Dye-sensitized Solar Cells. *Dyes Pigm.* **2011**, *88* (1), 75−83.
(29) Mathew, S.; Iijima, H.; Toude, Y.; Umeyama, T.; Matano, Y.; Ito, S.; Tkachenko, N. V.; Lemmetyinen, H.; Imahori, H. Optical, Electrochemical, and Photovoltaic Effects of an Electron-Withdrawing Tetrafluorophenylene Bridge in a Push-Pull Porphyrin Sensitizer Used for Dye-Sensitized Solar Cells. *J. Phys. Chem. C* **2011**, *115* (29), 14415−14424.
(30) Brennan, B. J.; Portoles, M. J. L.; Liddell, P. A.; Moore, T. A.; Moore, A. L.; Gust, D. Comparison of Silatrane, Phosphonic Acid, and Carboxylic Acid Functional Groups for Attachment of Porphyrin Sensitizers to TiO_2 in Photoelectrochemical Cells. *Phys. Chem. Chem. Phys.* **2013**, *15* (39), 16605−16614.
(31) Bessho, T.; Zakeeruddin, S. M.; Yeh, C. Y.; Diau, E. W.; Gratzel, M. Highly Efficient Mesoscopic Dye-sensitized Solar Cells Based on Donor-acceptor-substituted Porphyrins. *Angew. Chem., Int. Ed.* **2010**, *49* (37), 6646−6649.
(32) Imahori, H.; Umeyama, T.; Ito, S. Large π-Aromatic Molecules as Potential Sensitizers for Highly Efficient Dye-Sensitized Solar Cells. *Acc. Chem. Res.* **2009**, *42* (11), 1809−1818.
(33) Karthikeyan, S.; Lee, J. Y. Zinc-Porphyrin Based Dyes for Dye-Sensitized Solar Cells. *J. Phys. Chem. A* **2013**, *117* (42), 10973−10979.
(34) Li, X.-Y.; Zhang, C.-R.; Yuan, L.-H.; Zhang, M.-L.; Chen, Y.-H.; Liu, Z.-J. A Comparative Study of Porphyrin Dye Sensitizers YD2-o-C8, SM315 and SM371 for Solar Cells: the Electronic Structures and Excitation-related Properties. *Eur. Phys. J. D* **2016**, *70* (10), 211.
(35) Favereau, L.; Warnan, J.; Anne, F. B.; Pellegrin, Y.; Blart, E.; Jacquemin, D.; Odobel, F. Diketopyrrolopyrrole-zinc Porphyrin, a Tuned Panchromatic Association for Dye-sensitized Solar Cells. *J. Mater. Chem. A* **2013**, *1* (26), 7572−7575.
(36) Bauernschmitt, R.; Ahlrichs, R. Treatment of Electronic Excitations Within the Adiabatic Approximation of Time Dependent Density Functional Theory. *Chem. Phys. Lett.* **1996**, *256* (4−5), 454−464.
(37) Stratmann, R. E.; Scuseria, G. E.; Frisch, M. J. An Efficient Implementation of Time-dependent Density-functional Theory for the Calculation of Excitation Energies of Large Molecules. *J. Chem. Phys.* **1998**, *109* (19), 8218−8224.
(38) Casida, M. E.; Jamorski, C.; Casida, K. C.; Salahub, D. R. Molecular Excitation Energies to High-lying Bound States from Time-dependent Density functional Response Theory: Characterization and Correction of the Time- dependent Local Density Approximation Ionization Threshold. *J. Chem. Phys.* **1998**, *108* (11), 4439−4449.
(39) Yanai, T.; Tew, D. P.; Handy, N. C. A New Hybrid Exchange−correlation Functional Using the Coulomb-attenuating Method (CAM-B3LYP). *Chem. Phys. Lett.* **2004**, *393* (1−3), 51−57.
(40) Bernini, C.; Zani, L.; Calamante, M.; Reginato, G.; Mordini, A.; Taddei, M.; Basosi, R.; Sinicropi, A. Excited State Geometries and Vertical Emission Energies of Solvated Dyes for DSSC: A PCM/TD-DFT Benchmark Study. *J. Chem. Theory Comput.* **2014**, *10* (9), 3925−3933.
(41) Zhang, C.-R.; Liu, L.; Zhe, J.-W.; Jin, N.-Z.; Yuan, L.-H.; Chen, Y.-H.; Wei, Z.-Q.; Wu, Y.-Z.; Liu, Z.-J.; Chen, H.-S. Comparative Study on Electronic Structures and Optical Properties of Indoline and Triphenylamine Dye Sensitizers for Solar Cells. *J. Mol. Model.* **2013**, *19* (4), 1553−1563.
(42) High, J. S.; Virgil, K. A.; Jakubikova, E. Electronic Structure and Absorption Properties of Strongly Coupled Porphyrin−Perylene Arrays. *J. Phys. Chem. A* **2015**, *119* (38), 9879−9888.
(43) Li, X.-Y.; Zhang, C.-R.; Wu, Y.-Z.; Zhang, H.-M.; Wang, W.; Yuan, L.-H.; Yang, H.; Liu, Z.-J.; Chen, H.-S. The Role of Porphyrin-Free-Base in the Electronic Structures and Related Properties of N-Fused Carbazole-Zinc Porphyrin Dye Sensitizers. *Int. J. Mol. Sci.* **2015**, *16* (11), 27707−27720.
(44) Zhang, C.-R.; Han, L.-H.; Zhe, J.-W.; Jin, N.-Z.; Shen, Y.-L.; Gong, J.-J.; Zhang, H.-M.; Chen, Y.-H.; Liu, Z.-J. The Role of Terminal Groups in Electronic Structures and Related Properties: The Case of Push−pull Porphyrin Dye Sensitizers for Solar Cells. *Comput. Theor. Chem.* **2014**, *1039*, 62−70.
(45) Francl, M. M.; Pietro, W. J.; Hehre, W. J.; Binkley, J. S.; Gordon, M. S.; DeFrees, D. J.; Pople, J. A. Self-consistent Molecular Orbital Methods. XXIII. A Polarization-type Basis Set for Second-row Elements. *J. Chem. Phys.* **1982**, *77* (7), 3654−3665.
(46) Jacquemin, D.; Perpète, E. A.; Ciofini, I.; Adamo, C. Accurate Simulation of Optical Properties in Dyes. *Acc. Chem. Res.* **2009**, *42* (2), 326−334.
(47) Pastore, M.; Mosconi, E.; De Angelis, F.; Grätzel, M. A Computational Investigation of Organic Dyes for Dye-Sensitized Solar Cells: Benchmark, Strategies, and Open Issues. *J. Phys. Chem. C* **2010**, *114* (15), 7205−7212.
(48) Barone, V.; Cossi, M. Quantum Calculation of Molecular Energies and Energy Gradients in Solution by a Conductor Solvent Model. *J. Phys. Chem. A* **1998**, *102* (11), 1995−2001.
(49) Frisch, M. J.; Trucks, G. W.; Schlegel, H. B.; Scuseria, G. E.; Robb, M. A.; Cheeseman, J. R.; Scalmani, G.; Barone, V.; Mennucci, B.; Petersson, G. A.; et al. *Gaussian09*, Revision C.01; Gaussian, Inc.: Wallingford, CT, 2010.
(50) Marcus, R. A. Electron Transfer Reactions in Chemistry. Theory and Experiment. *Rev. Mod. Phys.* **1993**, *65* (3), 599−610.
(51) Preat, J.; Michaux, C.; Jacquemin, D.; Perpète, E. A. Enhanced Efficiency of Organic Dye-Sensitized Solar Cells: Triphenylamine Derivatives. *J. Phys. Chem. C* **2009**, *113* (38), 16821−16833.
(52) Katoh, R.; Furube, A.; Yoshihara, T.; Hara, K.; Fujihashi, G.; Takano, S.; Murata, S.; Arakawa, H.; Tachiya, M. Efficiencies of Electron Injection from Excited N3 Dye into Nanocrystalline Semiconductor (ZrO_2, TiO_2, ZnO, Nb_2O_5, SnO_2, In_2O_3) Films. *J. Phys. Chem. B* **2004**, *108* (15), 4818−4822.
(53) Zhang, C.-R.; Ma, J.-G.; Zhe, J.-W.; Jin, N.-Z.; Shen, Y.-L.; Wu, Y.-Z.; Chen, Y.-H.; Liu, Z.-J.; Chen, H.-S. The Electronic Structure Engineering of Organic Dye Sensitizers for Solar Cells: The Case of JK Derivatives. *Spectrochim. Acta, Part A* **2015**, *150*, 855−866.
(54) Asbury, J. B.; Wang, Y.-Q.; Hao, E.; Ghosh, H. N.; Lian, T. Evidences of Hot Excited State Electron Injection from Sensitizer Molecules to TiO_2 Nanocrystalline Thin Films. *Res. Chem. Intermed.* **2001**, *27* (4−1), 393−406.
(55) Boschloo, G.; Hagfeldt, A. Characteristics of the Iodide/Triiodide Redox Mediator in Dye-Sensitized Solar Cells. *Acc. Chem. Res.* **2009**, *42* (11), 1819−1826.

DOI: 10.1021/acs.jpca.6b12979
J. Phys. Chem. A 2017, 121, 2655−2664

(56) Zhang, C.-R.; Liu, L.; Liu, Z.-J.; Shen, Y.-L.; Sun, Y.-T.; Wu, Y.-Z.; Chen, Y.-H.; Yuan, L.-H.; Wang, W.; Chen, H.-S. Electronic Structures and Optical Properties of Organic Dye Sensitizer NKX Derivatives for Solar Cells: A Theoretical Approach. *J. Mol. Graphics Modell.* **2012**, *38* (0), 419−429.
(57) Zhang, C.-R.; Liu, Z.-J.; Chen, Y.-H.; Chen, H.-S.; Wu, Y.-Z.; Feng, W.; Wang, D.-B. DFT and TD-DFT Study on Structure and Properties of Organic Dye Sensitizer TA-St-CA. *Curr. Appl. Phys.* **2010**, *10* (1), 77−83.
(58) Kuss-Petermann, M.; Wenger, O. S. Increasing Electron-Transfer Rates with Increasing Donor-Acceptor Distance. *Angew. Chem., Int. Ed.* **2016**, *55* (2), 815−819.
(59) Zhang, C.-R.; Han, L.-H.; Zhe, J.-W.; Jin, N.-Z.; Wang, D.-B.; Wang, X.; Wu, Y.-Z.; Chen, Y.-H.; Liu, Z.-J.; Chen, H.-S. Tuning the Electronic Structures and Related Properties of Ruthenium-based Dye Sensitizers by Ligands: A Theoretical Study and Design. *Comput. Theor. Chem.* **2013**, *1017*, 99−108.
(60) Zhang, C.-R.; Liu, Z.-J.; Sun, Y.-T.; Shen, Y.-L.; Chen, Y.-H.; Liu, Y.-J.; Wang, W.; Zhang, H.-M. Electronic Structures and Absorption Properties of Three Kinds of Ruthenium Dye Sensitizers Containing Bipyridine-pyrazolate for Solar Cells. *Spectrochim. Acta, Part A* **2011**, *79* (5), 1843−1848.
(61) Feng, J.; Jiao, Y.; Ma, W.; Nazeeruddin, M. K.; Gratzel, M.; Meng, S. First Principles Design of Dye Molecules with Ullazine Donor for Dye Sensitized Solar Cells. *J. Phys. Chem. C* **2013**, *117* (8), 3772−3778.
(62) Ruhle, S.; Greenshtein, M.; Chen, S. G.; Merson, A.; Pizem, H.; Sukenik, C. S.; Cahen, D.; Zaban, A. Molecular Adjustment of the Electronic Properties of Nanoporous Electrodes in Dye-sensitized Solar Cells. *J. Phys. Chem. B* **2005**, *109* (40), 18907−18913.
(63) Kim, B.-G.; Zhen, C.-G.; Jeong, E. J.; Kieffer, J.; Kim, J. Organic Dye Design Tools for Efficient Photocurrent Generation in Dye-Sensitized Solar Cells: Exciton Binding Energy and Electron Acceptors. *Adv. Funct. Mater.* **2012**, *22* (8), 1606−1612.
(64) Gregg, B. A. Excitonic Solar Cells. *J. Phys. Chem. B* **2003**, *107* (20), 4688−4698.
(65) Scholes, G. D.; Rumbles, G. Excitons in nanoscale systems. *Nat. Mater.* **2006**, *5* (9), 683−696.

DOI: 10.1021/acs.jpca.6b12979
J. Phys. Chem. A 2017, 121, 2655−2664